symmetry

MDPI

Article

Evolving Hybrid Cascade Neural Network Genetic Algorithm Space–Time Forecasting

Rezzy Eko Caraka [1,2,*], Hasbi Yasin [3], Rung-Ching Chen [4,*], Noor Ell Goldameir [5], Budi Darmawan Supatmanto [6], Toni Toharudin [7], Mohammad Basyuni [8,*], Prana Ugiana Gio [9] and Bens Pardamean [2,10]

[1] Faculty of Economics and Business, Campus UI Depok, Universitas Indonesia, Depok 16426, Indonesia
[2] Bioinformatics and Data Science Research Center, Bina Nusantara University, Jakarta 11480, Indonesia; bpardamean@binus.edu
[3] Department of Statistics, Diponegoro University, Semarang 50275, Indonesia; hasbiyasin@live.undip.ac.id
[4] Department of Information Management, College of Informatics, Chaoyang University of Technology, Taichung 41349, Taiwan
[5] Department of Mathematics, Riau University, Pekanbaru 28293, Indonesia; noorellgoldameir@lecturer.unri.ac.id
[6] Weather Modification Technology Center, Agency for the Assessment and Application of Technology (BPPT), Jakarta 10340, Indonesia; budi.darmawan@bppt.go.id
[7] Department of Statistics, Padjadjaran University, Bandung 16426, Indonesia; toni.toharudin@unpad.ac.id
[8] Department of Forestry, Faculty of Forestry, Universitas Sumatera Utara, Medan 20155, Indonesia
[9] Department of Mathematics, Universitas Sumatera Utara, Medan 20155, Indonesia; prana@usu.ac.id
[10] Computer Science Department, Bina Nusantara University, Jakarta 11480, Indonesia
[*] Correspondence: rezzy.eko@ui.ac.id (R.E.C.); crching@cyut.edu.tw (R.-C.C.); m.basyuni@usu.ac.id (M.B.)

check for updates

Citation: Caraka, R.E.; Yasin, H.; Chen, R.-C.; Goldameir, N.E.; Supatmanto, B.D.; Toharudin, T.; Basyuni, M.; Gio, P.U.; Pardamean, B. Evolving Hybrid Cascade Neural Network Genetic Algorithm Space–Time Forecasting. *Symmetry* **2021**, *13*, 1158. https://doi.org/10.3390/sym13071158

Academic Editor: José Carlos R. Alcantud

Received: 7 May 2021
Accepted: 24 June 2021
Published: 28 June 2021

Abstract: Design: At the heart of time series forecasting, if nonlinear and nonstationary data are analyzed using traditional time series, the results will be biased. At the same time, if just using machine learning without any consideration given to input from traditional time series, not much information can be obtained from the results because the machine learning model is a black box. Purpose: In order to better study time series forecasting, we extend the combination of traditional time series and machine learning and propose a hybrid cascade neural network considering a metaheuristic optimization genetic algorithm in space–time forecasting. Finding: To further show the utility of the cascade neural network genetic algorithm, we use various scenarios for training and testing while also extending simulations by considering the activation functions SoftMax, radbas, logsig, and tribas on space–time forecasting of pollution data. During the simulation, we perform numerical metric evaluations using the root-mean-square error (RMSE), mean absolute error (MAE), and symmetric mean absolute percentage error (sMAPE) to demonstrate that our models provide high accuracy and speed up time-lapse computing.

Keywords: cascade neural network; space–time; forecasting; genetic algorithm; particulate matter

1. Introduction

Pollution describes the appearance and retention of the regular circulation of material, fine particles, biomaterial, and energy, or a deterioration technique or atmospheric change, which also has or may have significantly negative effects on human beings or the natural environment. Air pollutants are exhaust gases, particulate matter compounds, solid particulate matter, and other substances that emanate into the air, threatening the health of the community and damaging the environment. Air pollutants can be classified into smog and soot, pollution from contaminated air, greenhouse gas emissions, pollen, and mold.

PM refers to particulate matter, also known as particulate emissions. PM comprises aggregated rigid particles and atmospheric fluid droplets. Some are large enough or visible enough to be seen with the naked eye, and others are so small that they can only be seen with electron microscopes. PM_{10} and $PM_{2.5}$ are some classes of these particulate pollutants [1–4]. Let us consider a hair: the mean diameter of a single human hair is approximately 70 micrometers. This is roughly 28 times the diameter of $PM_{2.5}$. The diameter of particulate matter in PM_{10} is 10 micrometers or below. Similarly, $PM_{2.5}$ is normally particles of diameter 2.5 micrometers or below. Both PM_{10} and $PM_{2.5}$ are inhalable. We can thus imagine how tiny 2.5 and 10 micrometers are.

PM can be made up of various chemicals, including sulfur dioxide (SO_2) and nitrogen oxides, originating in PM (NOx) [5–7]. All this can be found as a product of building materials, farms, explosions, power stations, industry, and vehicles. PM is seriously damaging, as described above, as it may be opaque and small enough to be inhaled into the lungs or even into the circulation. Therefore, PM contamination affects the cardiovascular system and can cause fatal illnesses such as cardiovascular diseases, erratic heartbeat, and worsening asthma [8–10].

The estimation of future air pollution is an important task because it can be used to manage risk. The Artificial Neural Network (ANN) is the most frequently used among many data-driven applications and is a modern method and an effective paradigm for predicting and forecasting variables in the management of contamination risk due to intrinsic contaminant source uncertainties using quality data [11,12]. ANNs were inspired by the human brain's biochemical neural networks. McCulloch and Pitts in (1943) [13] initially developed a mathematically dependent model and referred to it as a threshold logic computing model for neural networks [14–19].

The neurons are important in the neural network's operating condition, they are very connected and share signals with one another, whether it is a neuron or node. Every layer consists of one or more simple elements called neurons. As the input data are transferred to the input layer, they bind with the weight and are nonlinearized by the activation function; the process of being sent to the next neuron is replicated before the final outcome is achieved. Each new neuron consists of one weight and one activation function [20,21]. The connectivity of neurons is handled by utilizing established inputs and outputs and is seen in an organized way in the ANN. The training phase is represented as a trial-and-error process to select the number of neurons [22,23]. The intensity of these interconnections is adapted to the known pattern using an error convergence technique. In this article, a cascade neural network procedure based on the genetic algorithm is developed for space–time forecasting data. This article is organized as follows: In Section 2, we review the training using the cascade neural network and employ a genetic algorithm. The performance is examined in Section 3 via simulation studies and analysis of four benchmark real datasets of air pollution data. Finally, Section 4 presents our conclusions.

2. Methods

2.1. Cascade Neural Network

The neural network's environment is uncertain. It is presumed that the teacher and the neural network are linked to an environmental testing vector, as an example. Because of the integrated experience, the teacher is capable of responding to this training vector in the algorithm. In fact, the appropriate outcome is the optimal response of the neural network. The key property of a neural network is the network's capacity to improve performance by learning from its experience [24]. Based on how well the neural networks operate, the networks are divided into supervised learning networks and unsupervised learning networks, otherwise termed teacher learning and teacher-free learning. Structurally, we may think of the teacher as having information about the environment, portrayed by a variety of samples of input and output [25,26].

The network parameters are managed according to the cumulative effect of the training vector, mostly with error signals. Meanwhile, each error signal should be specified as the gap between the requested response and the network's actual response. This modification is made step by step in order to rapidly mimic the teacher in the neural network, with the emulation in any mathematical context assumed to be ideal. This transfers awareness of the teacher's setting to the neural network as thoroughly as possible by preparation [27]. If this is achieved, then we can dispense with the teacher and encourage the neural network to deal entirely with the environment. Throughout the supervised NN model, input vectors and suitable target vectors are used to update the parameters; before a function can be approximated, input features should be tied to specific output vectors and the information that can be processed should be properly identified [28,29].

The most famous and typical algorithm for neural network training is the context of an error, the main principle of which is that an error in the hidden neurons is calculated by propagation of the error in the output layer neurons. The traditional backpropagation algorithm uses two input and learning processes. Vectors or patterns are displayed in the input layer in feedforward operation, and each neuron throughout the hidden layer is measured in the activation with one neuron net_j. The input vector dot product including neuron weight in the hidden layer is represented in Equation (1):

$$net_j = \sum_{i=1}^{N_i} x_i w_{ij}^{I-H} + b_{ij} = \sum_{i=0}^{N_i} x_i w_{ij}^{I-H} \tag{1}$$

where N_i is the input vector dimension, and i and j are neuron indices in the layer input and in the hidden layer, respectively. The weight value between the input vectors and neurons in the hidden layer is w_{ij}^{I-H}. The weight value of bias in the hidden layer is b_{ij} and is usually assumed to be $b_{ij} = w_{0j}^{I-0}$, $x_0 = 1$. By substituting net_j into activation function φ_1, θ_j is calculated. In the activation of a single neuron, each neuron in the output layer computes net_k, which is the dot product of θ_j and the neuron weight in the output layer, represented in Equations (2) and (3).

$$\theta_j = \varphi_1\left(net_j\right) \tag{2}$$

$$net_k = \sum_{j=1}^{N_H} \theta_j w_{jk}^{H-0} \tag{3}$$

In line with this, N_H is the number of neurons in the hidden layer and k is the index of a neuron in the output layer. The weight value of neurons between the hidden layer and output layer is described as w_{jk}^{H-0}. We can substitute net_k into activation function φ_2 to output y_k, represented in Equation (4).

$$y_k = \varphi_2(net_k) \tag{4}$$

$$y_k = \varphi_2\left(\sum_{j=1}^{N_H} \theta_j w_{jk}^{H-0}\right) \tag{5}$$

$$y_k = \varphi_2\left(\sum_{j=0}^{N_H} w_{jk}^{H-0}\left(\sum_{i=0}^{N_i} x_j w_{ij}^{I-H}\right)\right) \tag{6}$$

Regarding Equations (4) and (5), the entire collection of weights is updated to ensure that y_k is near the target output value of t_k by propagating the E_r error of the output layer neurons throughout the learning phase. Although a variety of output functions are available to evaluate the error, the squared error is commonly used, represented in Equation (7).

$$E_r = \sum_{k=1}^{N_0} (t_k - y_k)^2 \tag{7}$$

2.2. Genetic Algorithm

Biological variation and its basic processes were clarified by Darwin's (2002) evolutionary theory [30]. Natural selection is fundamental to what is often referred to as the macroscopic understanding of evolution. In an environment where only a finite number of humans will survive, and given the basic tendency of people to multiply, selection is necessary if people do not have an accelerated population [31,32]. This evolution favors people who bid more successfully for the given resources. In other words, they are better suited or adapted to the climate, recognized as global best survival [33].

Selection on the basis of competition is one of the two pillars of the mechanism of evolution. The other main influence comes as a function of phenotypical differences in the populations. The phenotype is an individual's physical and behavioral characteristics that assess their fitness in terms of their exposure to the surrounding environment. That individual represents a specific combination of environmental assessment phenotypic characteristics. These characteristics are inherited by the offspring of the individual if evaluated with favor; otherwise, the offspring is discarded. Charles Darwin's insight was that slight, spontaneous phenotype changes occur across ages [34–36].

New combinations of phenotype arise and are assessed by these mutations. That is the fundamental basis of the genetic algorithm: With a population of individuals, constraints on the environment lead to natural selection and survival of the population via roulette wheel selection, which results in an increase in the fitness of the population. A random collection of candidates can be generated [37]. Depending on this fitness, many of the best candidates are selected for the next generation using conjugation to seed the performance as an abstract fitness metric [38]. Cross-over and mutation give rise to a number of new offspring that fight for a position in the next generation on the basis of their fitness with old members of the population, before an organism of adequate efficiency is identified and until a previously determined computational threshold is exceeded [39,40]. In line with this, Algorithm 1 shows the scheme of the genetic algorithm. The scheme coincides with the generate-and-test algorithm type. The fitness function constitutes a heuristic estimate of an optimal solution, and the cross-over, mutation, and selection operators guide the search algorithm. The genetic algorithm has many characteristics that can support in the generating and testing of parents.

Algorithm 1. Scheme of the GA

```
INITIALIZE population and EVALUATE
while termination condition is not satisfied do
    SELECT parents
    CROSSOVER pairs of parents
    MUTATE the resulting offspring
    EVALUATE new candidates
    REPLACE individuals for the next generation
end while
```

2.3. Cascade Neural Network Genetic Algorithm

Backpropagation training algorithms based on other traditional optimization methods, such as the conjugating gradient and Newton process, have different variants. This same gradient descent approximation, the easiest and among the slowest, usually speeds up the conjugate gradient algorithm, as well as Newton's method [41,42]. We used genetic algorithms through this study. Each neuron weight between the hidden layer and the output layer should be updated, and the weight of the neurons here between the input and the hidden layer was adjusted [43]. The weight change between some of the hidden and output layers of the neuron is specified in Equation (8) with activation function $\varphi(x) = \frac{1}{x}$.

$$\frac{\partial E_r}{\partial w_{jk}^{H-0}} = \frac{\partial E_r}{\partial net_k} \cdot \frac{\partial net_k}{\partial w_{jk}^{H-0}}$$

$$\frac{\partial E_r}{\partial w_{jk}^{H-0}} = -(t_k - y_k) \cdot \varphi^2(net_k) \cdot \theta_j \tag{8}$$

The weight value of neurons was updated between the input and hidden layer as represented in Equation (9).

$$\frac{\partial E_r}{\partial w_{jk}^{I-H}} = \frac{\partial E_r}{\partial \theta_j} \cdot \frac{\partial \theta_j}{\partial net_k} \cdot \frac{\partial net_k}{\partial w_{jk}^{I-H}}$$

$$\frac{\partial E_r}{\partial w_{jk}^{I-H}} = \left[\frac{1}{2} \sum_{k=1}^{N_0} (t_k - y_k)^2 \right] \cdot \frac{\partial \theta_j}{\partial net_k} \cdot \frac{\partial net_k}{\partial w_{jk}^{I-H}}$$

$$\frac{\partial E_r}{\partial w_{jk}^{I-H}} = \left[(t_k - y_k)^2 \cdot \frac{\partial y_k}{\partial \theta_j} \right] \cdot \frac{\partial \theta_j}{\partial net_k} \cdot \frac{\partial net_k}{\partial w_{jk}^{I-H}}$$

$$\frac{\partial E_r}{\partial w_{jk}^{I-H}} = \left[(t_k - y_k)^2 \cdot \frac{\partial y_k}{\partial net_k} \frac{\partial net_k}{\partial \theta_j} \right] \cdot \frac{\partial \theta_j}{\partial net_j} \cdot \frac{\partial net_j}{\partial w_{ij}^{I-H}}$$

$$\frac{\partial E_r}{\partial w_{jk}^{I-H}} = - \sum_{k=1}^{N_0} \left[(t_k - y_k) \cdot \varphi_2(net_k) \cdot w_{jk}^{H-0} \right] \cdot \varphi_1\left(net_j\right) \cdot x_i \tag{9}$$

With backpropagation, the input data are repeatedly presented to the neural network. With each presentation, the output of the neural network is compared to the desired output, and the error is computed. This error is then backpropagated through the neural network and used to adjust the weights such that the error decreases with each iteration; the neural network thus gets closer and closer to producing the desired output, represented in Equation (10).

$$w(h+1) = w(h) + \Delta w(h) \tag{10}$$

Algorithm 2 shows the function cascade neural network. However, the context backpropagation of each input datum is continuously shown to the neural network, with every representation comparing the output of the neural network to the requested output and computing the error; these errors provide context to the neural network and are used to update the weights to reduce its error for each iteration, as well as the genetic algorithm, allowing new generation of the neural network.

Algorithm 2. Function Cascade Neural Network

```
input $n_h$, $m$, $o$
set $k = 0$
calculate Cascade Weighted
$k = 0$;
for $i = 1:nh$
    for $j = 1:m$
        $k = k + 1$;
        $Wi1(i,j) = W(k)$;
    end
end
calculate weighted input and output
for $i = 1:o$
    for $j = 1:m$
        $k = k + 1$;
        $Wi2(i,j) = W(k)$;
    end
end
calculate weighted Bias Input
for $i = 1:nh$
    $k = k + 1$;
    $Wbi(i,1) = W(k)$;
end
calculate weighted output
for $i = 1:o$
    for $j = 1:nh$
        $k = k + 1$;
        $Wo(i,j) = W(k)$;
    end
end
calculate weighted Bias Output
for $i = 1:o$
    $k = k + 1$;
    $Wbo(i,1) = W(k)$;
end
```

3. Simulation and Results

3.1. Construction of VAR-Cascade

There exist few guidelines for building a neural network model for time series. One of them considers time series as a nonlinear function of several past observations and random errors. Since air pollution data are known to be nonlinear time series data, we selected this method as a benchmark for forecasting. Equation (11) represents the time series models:

$$y_t = f[(z_{t-1}, z_{t-2}, \ldots, z_{t-m}),\ (e_{t-1}, e_{t-2}, \ldots,\ e_{t-n})] \tag{11}$$

where f is a nonlinear function determined by the neural network, $z_t = (1-B)^d\, y_t$, and d represents the order difference. Also, the residuals at time t are defined as e_t, and m and n are integers. Equation (12) shows that, initially, the VAR model is fitted in order to generate the residuals e_t. A neural network is then used to model the nonlinear and linear relations in excess and the original results [22,44,45].

$$z_t = w_0 + \sum_{j=1}^{Q} w_j \cdot g\left(w_{0j} + \sum_{i=1}^{p} w_{ij} \cdot z_{t-i} + \sum_{i=p+1}^{p+q} w_{ij} \cdot e_{t+p-i} \right) + \epsilon_t \tag{12}$$

Here, $w_{ij}(i = 0, 1, 2, \ldots, p + q, j = 1, 2, \ldots, Q)$ and $w_j(j = 0, 1, 2, 3, \ldots, Q)$ are connection weights and p, q, Q are integers that should be determined in the design process of the cascade neural network. The values of p and q are determined by the underlying properties of the data. If the data are just nonlinear, they only consist of nonlinear structures; then, q can be 0 since the Box–Jenkins method is a linear model that cannot simulate nonlinear interaction. Suboptimal methods may be used in a hybrid model, but suboptimality does not change the functional characteristics of the hybrid approach [17,46–48].

The interpretation of time series requires quantification of the vector dynamic response with time shifts. The main feature of this method is to forecast potential values using recent qualities of a variable, often referred to as lagged values [49]. Commonly, the latest values influence the estimation of a potential value most strongly [50,51]. A single scalar variable is frequently expressed in series data evaluation of a self-regression where future values are estimated based on the weighted total of pre-set lagged values. This variable relies on its own previous values as well as the previous values for many other variables in the much more specific multivariate case [52–54].

3.2. Study Area

The study areas were Taipei, Hsinchu, Taichung, and Kaohsiung city, with pollution data consisting of nitrogen oxide (NOx), atmospheric $PM_{2.5}$, atmospheric PM_{10}, and sulfur dioxide (SO_2) levels. Furthermore, the locations of these areas were as established by the Taiwan Environmental Protection Administration Executive Yuan. Table 1 shows statistical summaries of the amounts of air pollution at the four studied locations. The findings typically demonstrate that Taichung has higher concentrations of PM_{10}, $PM_{2.5}$, and NO_X, but in Kaohsiung, SO_2 is the greatest pollutant. Figure 1 shows an overview of the genetic algorithm's training and evaluation phases. Because each type of air pollutant has a different distribution, we trained the same models for each dataset using the same model architecture.

Table 1. Descriptive statistics.

Pollution	Location	N	Mean	SE Mean	StDev	Variance	Minimum	Q_1	Median	Q_3	Maximum	Range
PM_{10}	TAICHUNG	3632	50.642	0.419	24.949	622.476	5	32	45.5	65	173	168
	TAIPEI	3632	21.244	0.208	12.412	154.052	1	12	19	27	100	99
	HSINCHU	3632	22.46	0.219	13.135	172.521	1	13	19	29	103	102
	KAOHSIUNG	3632	31.719	0.31	18.477	341.414	1	17	29	44	123	122
SO_2	TAICHUNG	3632	2.8706	0.017	1.0208	1.042	0	2.2	2.7	3.4	9.3	9.3
	TAIPEI	3632	2.9835	0.0263	1.5742	2.4781	0.4	1.9	2.6	3.7	16.2	15.8
	HSINCHU	3632	2.6778	0.0186	1.1125	1.2377	0.1	1.9	2.5	3.2	13.2	13.1
	KAOHSIUNG	3632	5.3129	0.0515	3.0833	9.5066	0	3.3	4.5	6.4	33.8	33.8
$PM_{2.5}$	TAICHUNG	3632	26.623	0.264	15.66	245.244	1	15	23	35	106	105
	TAIPEI	3632	23.635	0.203	12.161	147.892	3.97	15.107	20.84	29.023	109.83	105.86
	HSINCHU	3632	18.179	0.13	7.763	60.265	0.63	13.04	16.34	21.102	76.72	76.09
	KAOHSIUNG	3632	23.854	0.163	9.747	95.014	5.27	16.49	21.495	29.697	68.96	63.69
NO_X	TAICHUNG	3632	22.944	0.171	10.26	105.269	4.35	15.23	20.57	28.63	81.43	77.08
	TAIPEI	3632	6.196	0.106	6.315	39.874	0.09	1.85	4.15	8.28	65.14	65.05
	HSINCHU	3632	3.2786	0.0546	3.2643	10.6559	0	1.52	2.3	3.79	45.65	45.65

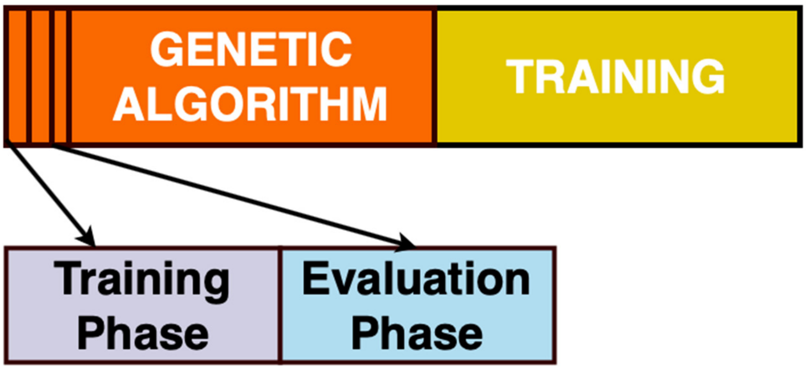

Figure 1. An overview of the genetic algorithm training and evaluation phases.

Samples for training were split in two, and alternating training and assessment were done in the first half of the samples. After this part was complete, the other half was used for forest training. Again, the first half was divided into smaller sections called stages. We perform simulations for ratios of 90:10, 80:20, 70:30, 60:40, and 50:50. In the training process, the training samples from the stepper were conditioned for all chromosomes, including new chromosomes of the previous level. Before the formation of the new chromosomes, all forests were educated in parallel. After all forests were qualified in the training part, genetic operators were used in the assessment part to calculate fitness values to operate in the genetic pool. This algorithm altered the substitute operator location to first and functioned only when a new chromosome was generated at the previous point.

3.3. Air Pollution Forecasting Using VAR-Cascade-GA

Poor air quality in Taiwan has mostly been identified as being a result of household burning, largely the source of greenhouse gas emissions. Taiwan's geography was observed to be a primary contributor towards its environmental problems, resulting in poor absorption and pollutant locking. Taipei, Taiwan's capital and most populous city, is surrounded by mountains, and advanced manufacturing offices all along the western and northern coastlines of Taiwan were also built near mountain ranges. In Section 3, we already discussed the construction step and simulation studies. Furthermore, during the construction stage of input, we employed the VAR pollution space–time dataset including Taichung (Y_1), Taipei (Y_2), Hsinchu (Y_3), and Kaohsiung (Y_4) in Taiwan.

Figure 2 shows that five hidden layers were used to create the model, and the ratio used was calculated by assessing the error values of the testing results shown in Table 2. During training and testing, $PM_{2.5}$ is represented in Figure 3, PM_{10} is represented in Figure 4, NO_X is represented in Figure 5, and SO_2 is represented in Figure 6. In this context, the cascade neural network genetic algorithm model can be used to study nonlinear and nonstationary data on air pollution. The metrics used to evaluate the test set's result were the root-mean-squared error (RMSE), mean absolute error (MAE), and symmetry mean absolute percentage (sMAPE) between the actual air pollution values and the predicted values. These are metrics that are commonly used in regression problems like our air pollution prediction. If all the metric values are smaller, then the model's performance is better [25].

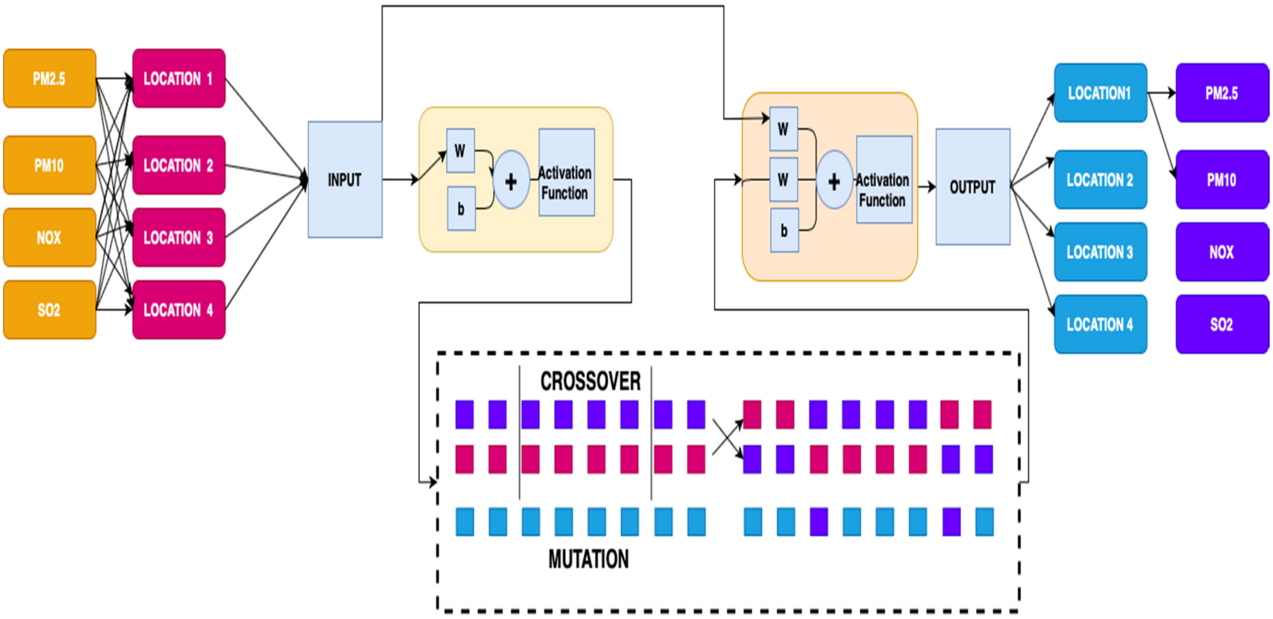

Figure 2. Space–time Cascade Neural Network with genetic algorithm, adopted by [22,36].

Table 2. Model comparison based on pollution.

Pollution	**Portion**	**Training**			**Testing**			**Average**			**Elapsed Time**
		RMSE	**MAE**	**SMAPE**	**RMSE**	**MAE**	**SMAPE**	**RMSE**	**MAE**	**SMAPE**	
PM$_{2.5}$	50:50	9.84	6.89	3.91	7.89	5.70	3.83	8.87	6.30	3.87	76.42
PM$_{10}$		13.53	9.57	3.84	11.37	8.05	3.86	12.45	8.81	3.85	71.86
NO$_X$		5.53	3.55	6.94	4.37	2.73	6.95	4.95	3.14	6.95	74.23
SO$_2$		1.72	1.18	3.60	1.15	0.80	3.61	1.44	0.99	3.61	75.51
PM$_{2.5}$	60:40	9.86	6.88	3.89	7.41	5.42	3.57	8.63	6.15	3.73	76.56
PM$_{10}$		13.49	9.54	3.76	10.67	7.57	3.56	12.08	8.55	3.66	75.24
NO$_X$		6.48	3.48	6.93	4.10	2.65	6.24	5.29	3.06	6.59	73.15
SO$_2$		1.65	1.13	3.48	1.07	0.80	3.43	1.36	0.97	3.46	76.13
PM$_{2.5}$	70:30	9.43	6.62	3.83	7.13	5.27	3.50	8.28	5.95	3.67	71.13
PM$_{10}$		13.30	9.29	3.74	10.09	7.13	3.74	11.70	8.21	3.74	77.87
NO$_X$		5.31	3.36	6.98	4.01	2.54	7.12	4.66	2.95	7.05	74.41
SO$_2$		1.60	1.09	3.36	1.00	0.77	3.41	1.30	0.93	3.38	80.90
PM$_{2.5}$	80:20	9.25	6.46	3.81	6.83	4.99	3.50	8.04	5.73	3.65	74.25
PM$_{10}$		13.10	9.07	3.74	9.19	6.56	4.13	11.14	7.82	3.93	74.25
NO$_X$		5.25	3.29	7.11	3.79	2.49	6.68	4.52	2.89	6.90	72.37
SO$_2$		1.54	1.05	3.42	0.92	0.70	3.36	1.23	0.88	3.39	80.24
PM$_{2.5}$	90:10 *	9.03	6.34	3.77	6.78	4.94	3.47	7.90	5.64	3.62	83.83
PM$_{10}$		12.77	8.85	3.77	8.02	5.93	4.09	10.40	7.39	3.93	75.00
NO$_X$		5.11	3.20	6.90	3.70	2.43	6.53	4.40	2.81	6.72	80.47
SO$_2$		1.48	1.10	3.37	0.80	0.62	2.77	1.14	0.86	3.07	71.71

Noted: Best simulation with low error (*) and yellow highlight represent the lowest value of each information pollution, accuracy measurement, and elapsed time.

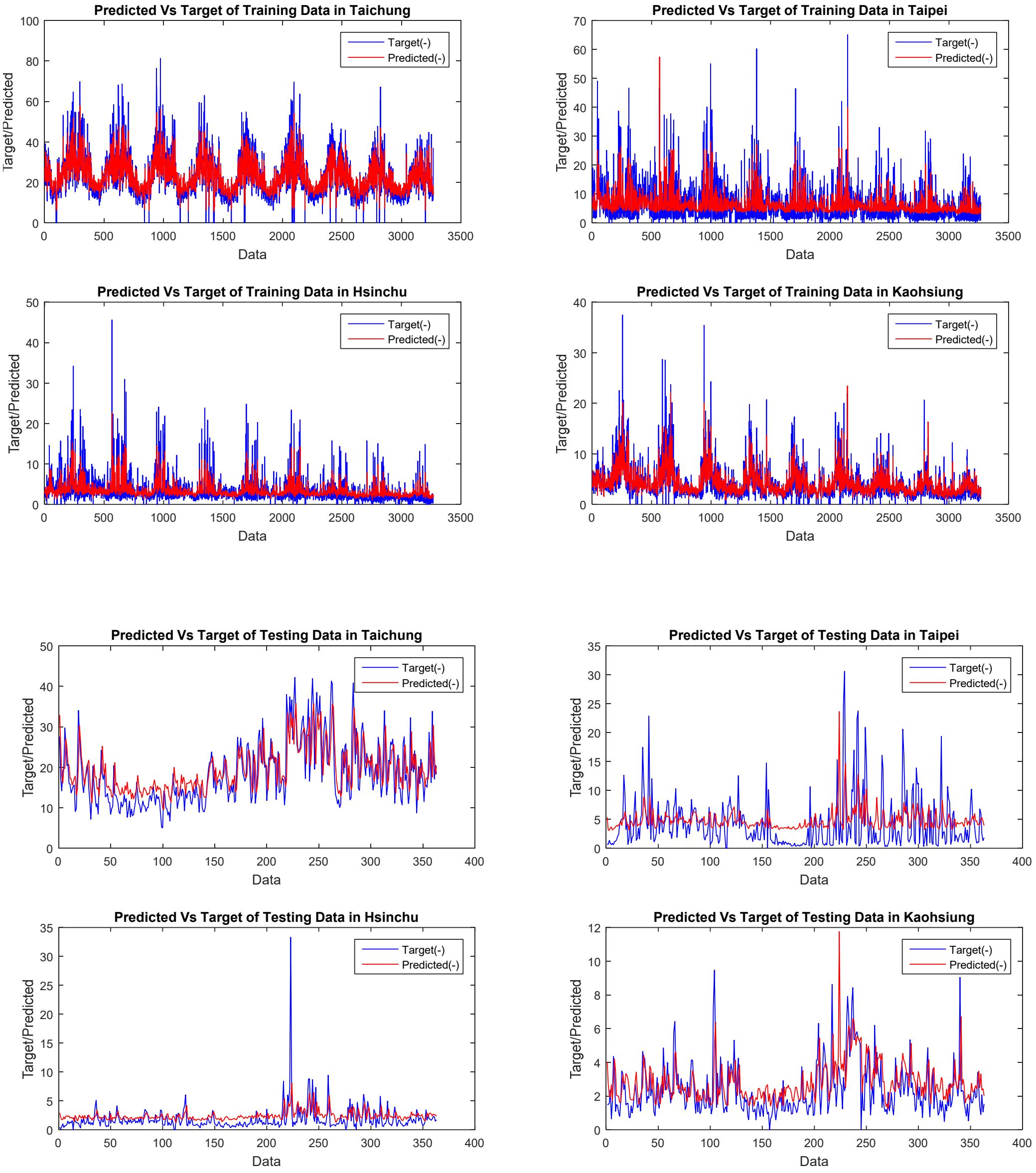
Predicted Vs Target of Training Data in Taichung

Predicted Vs Target of Training Data in Taipei

Predicted Vs Target of Training Data in Hsinchu

Predicted Vs Target of Training Data in Kaohsiung

Predicted Vs Target of Testing Data in Taichung

Predicted Vs Target of Testing Data in Taipei

Predicted Vs Target of Testing Data in Hsinchu

Predicted Vs Target of Testing Data in Kaohsiung

Figure 3. $PM_{2.5}$ data training of the CFNN using a genetic algorithm and backpropagation.

In the results, the cascade neural network genetic algorithm with ratio 90:10 provided lower RMSE, MAE, and sMAPE values for all variables. The optimum number of hidden neurons showing good performance in the test and validation results could then be selected. Using this model, a prediction of future air pollution was performed. In this study area, the air pollution levels in these four cities in Taiwan influence each other. However, the accuracy of prediction was not improved when we set the training and testing ratio to 80:20, 70:30, 60:40, or 50:50 in the same section. There are several training algorithms, such as backpropagation, Conjugate Gradient Powell–Beale (CGB), Broyden–Fletcher–Goldfarb (BFG), Levenberg–Marquardt (LM), and Scaled Conjugate Gradient (SCG). The rate of change in the error with respect to the connection weight including the error gradient is used as a path for training.

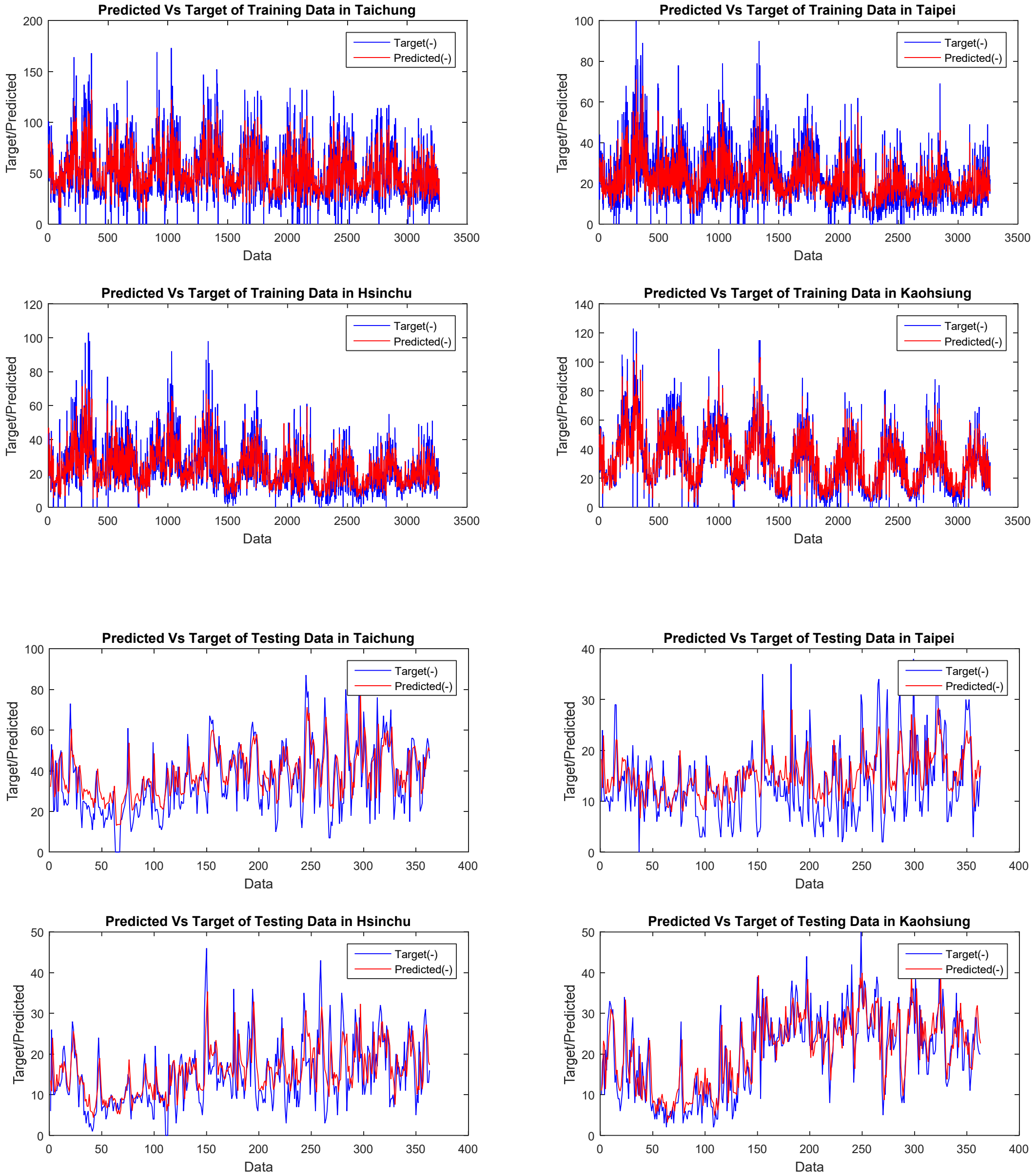
Predicted Vs Target of Training Data in Taichung

Predicted Vs Target of Training Data in Taipei

Predicted Vs Target of Training Data in Hsinchu

Predicted Vs Target of Training Data in Kaohsiung

Predicted Vs Target of Testing Data in Taichung

Predicted Vs Target of Testing Data in Taipei

Predicted Vs Target of Testing Data in Hsinchu

Predicted Vs Target of Testing Data in Kaohsiung

Figure 4. PM$_{10}$ data training of the CFNN using a genetic algorithm and backpropagation.

In order to measure the stage size to optimize performance, we used backpropagation and conducted a search along the conjugate or orthogonal path. Appropriately, we proved that this was the easiest way to train moderate feedback networks. That being said, some matrix multiplication is included in the processing for such issues as air pollution over time. The network is very wide in this research, so using backpropagation is a good way. When overfitting occurs, the transferability of the potential is significantly decreased. To suppress overfitting, methods such as so-called regularization are often used. L1 (L2) regularization adds the sum of the absolute (square) values of weights to the loss function, as in Equations (13) and (14), where Γ is the loss function and w_{jk}^{i} indicates the weights in the network. In addition, α is the scaling factor for the summation. N_H denotes the number of layers and N_i denotes the number of nodes in the ith layer.

$$\Gamma_{L1} = \Gamma + \alpha \sum_{i=1}^{N_H-1} \sum_{j=1}^{N_i} \sum_{k=1}^{N_{i+1}} \left| w_{jk}^{i} \right| \qquad (13)$$

$$\Gamma_{L2} = \Gamma + \alpha \sum_{i=1}^{N_H-1} \sum_{j=1}^{N_i} \sum_{k=1}^{N_{i+1}} \left(w^{i}_{jk}\right)^2 \tag{14}$$

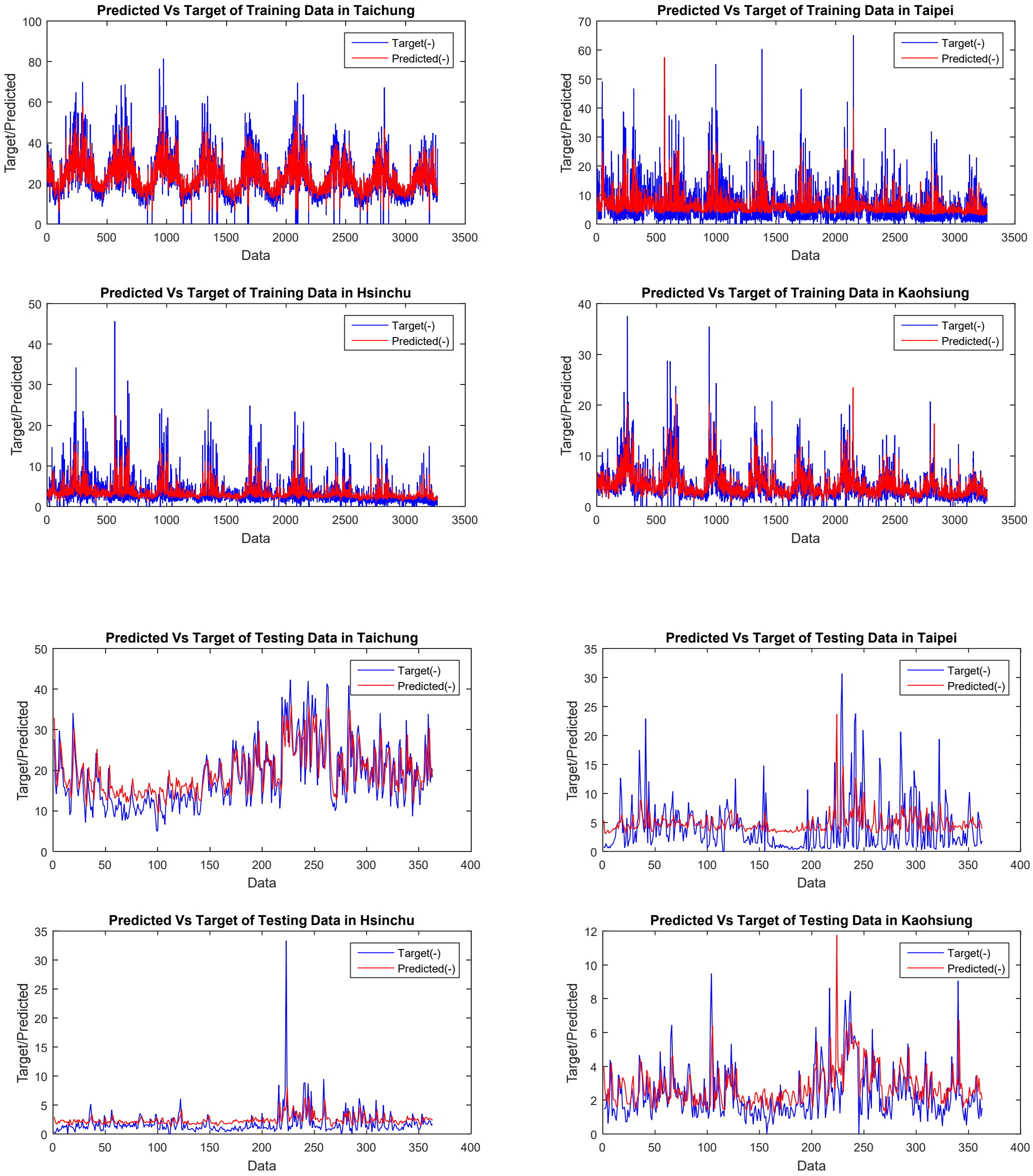

Figure 5. NO_x data training of the CFNN using a genetic algorithm and backpropagation.

3.4. Does the Activation Function Provide High Accuracy and Speed Up the Time Lapse?

Linear regression models work well throughout short-term predictions based on daily or weekly measurements in time series forecasting, but they cannot tackle nonlinearity in showing variables properly, not even for long-term predictions from seasonal or annual data series. Various machine learning methodologies have been introduced and used to simulate problems and provide predictions in environmental research, as machine efficiency has been evolving rapidly in the last decade. Despite its prominence and outstanding data accuracy, critical issues in the Artificial Neural Network are its propensity to overfit training data and inconsistency for short histories of training data. Several strategies for more effective and efficient preparation of NNs have been recommended. However, these are not simple and also have markedly poor accuracy.

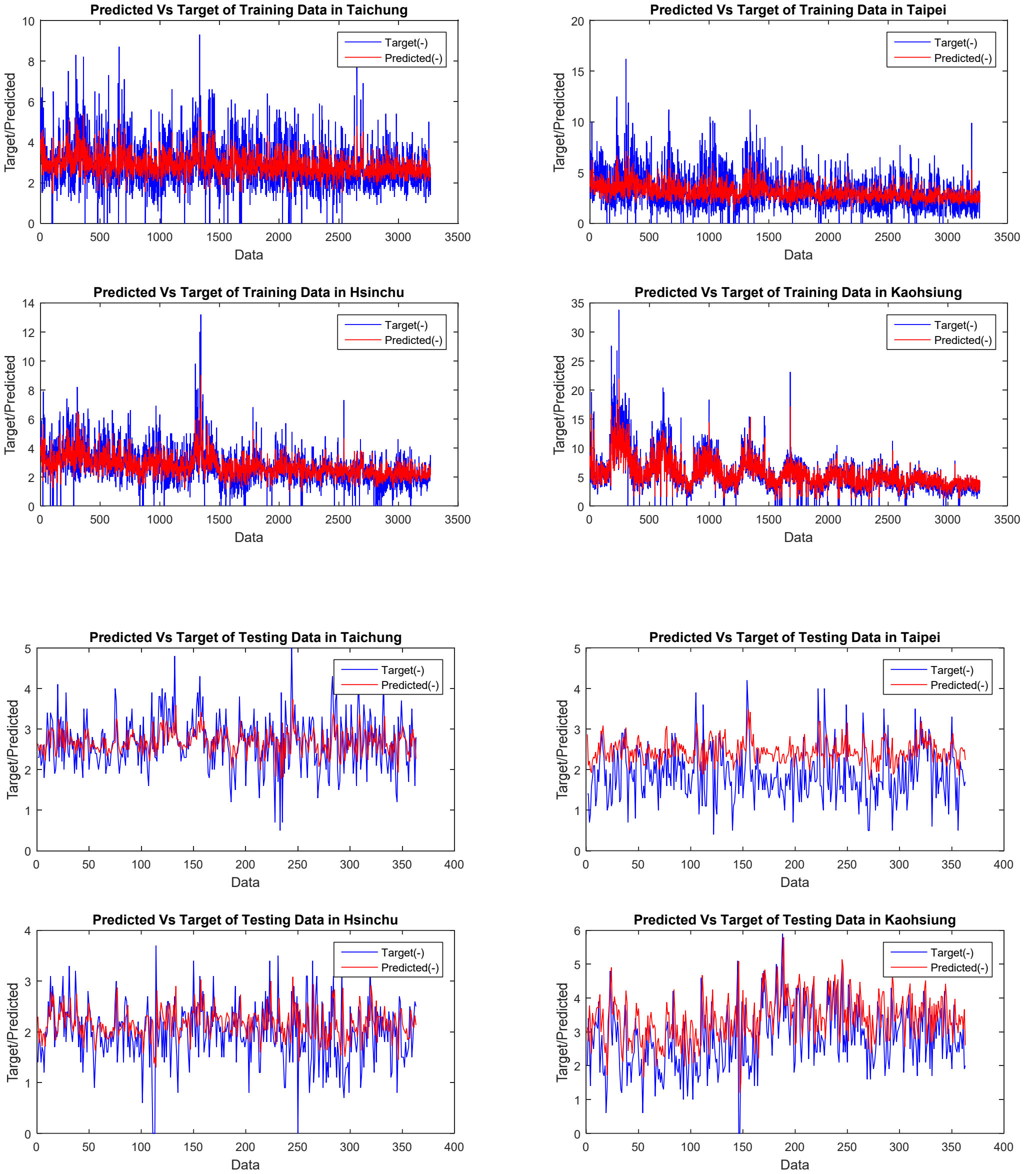

Figure 6. SO_2 data training of the CFNN using a genetic algorithm and backpropagation.

After the training and testing comparisons already discussed in Section 3.3, we considered proving the performance of the hybrid cascade neural network genetic algorithm when using other activation functions. Computational capabilities are increasing in the era of big data, high-performance computing, parallel processing, and cloud computing. In line with this, we address whether the activation function can improve accuracy and speed up the time lapse. Throughout the last decades, the machine learning domain, a branch of artificial intelligence, has gained popularity, and researchers in the area have led it to expand through various areas of human life. Machine learning is a part of research that employs statistics and computer science concepts to develop mathematical models used to execute large tasks such as estimation and inference [55]. These frameworks are collections of mathematical interactions between the system's inputs and outputs. A learning process entails predicting the model parameters so that the task can be executed effectively. To improve accuracy, researchers have conducted simulated comparisons using various activation functions. The most popular activation functions are SoftMax, tanh, ReLU, Leaky ReLU, sigmoid, and logsig [56–59].

As asserted, the activation function can be defined and applied to an ANN to assist the network in understanding various systems in data. Although contrasted to a neuron-based design seen in human brains, an activation function is essentially responsible for determining what neuron to trigger immediately [60]. Inside an ANN, the activation function is doing the same thing. All of this receives a prior nerve cell output signal and transforms it into a format which can be used as feedback to yet another cell. In this simulation, we used logsig in Equation (15), radbas in Equation (16), SoftMax in Equation (17), and tribas in Equation (18).

$$z_j = \frac{1}{1+\exp(-X_j)} \tag{15}$$

$$z(x) = \sum_{i=1}^{N} w_i \varphi(\|x - x_i\|) \tag{16}$$

$$\sigma(\vec{z})_i = \frac{e^{z_i}}{\sum_{j=1}^{K} e^{z_j}} \tag{17}$$

$$tri(x) = \Lambda(x) \overset{\text{def}}{=} \max(1 - |x|, 0) \tag{18}$$

Table 3 shows that the best activation function for PM_{10} was logsig, that for $PM_{2.5}$ was SoftMax, that for NO_X was radbas, and that for SO_2 was tribas. The SoftMax activation function provided a shorter time lapse than other activation functions.

Table 3. Combining activation functions with the Cascade Neural Network.

Pollution	Activation Function	Training			Testing			Average			Elapsed Time
		RMSE	MAE	SMAPE	RMSE	MAE	SMAPE	RMSE	MAE	SMAPE	
$PM_{2.5}$	logsig	9.02	6.30	3.77	6.77	4.94	3.54	7.90	5.62	3.66	78.03
PM_{10}		12.79	8.86	3.71	8.12	6.02	4.05	10.46	7.44	3.88	75.48
NO_X		5.04	3.15	6.84	3.79	2.43	6.62	4.42	2.79	6.73	72.43
SO_2		1.48	1.01	3.35	0.82	0.63	3.00	1.15	0.82	3.18	76.59
$PM_{2.5}$	radbas	9.06	6.37	3.80	6.80	5.00	3.51	7.93	5.69	3.66	80.97
PM_{10}		12.79	8.85	3.79	8.11	6.03	4.19	10.45	7.44	3.99	74.77
NO_X		5.09	3.16	6.83	3.75	2.40	6.19	4.42	2.78	6.51	82.35
SO_2		1.49	1.01	3.36	0.83	0.64	2.93	1.16	0.83	3.15	73.33
$PM_{2.5}$	SoftMax	9.07	6.35	3.78	6.70	4.91	3.46	7.89	5.63	3.62	75.47
PM_{10}		12.81	8.90	3.75	8.13	6.04	4.24	10.47	7.47	3.99	74.70
NO_X		5.11	3.19	7.12	3.64	2.35	6.23	4.38	2.77	6.67	72.11
SO_2		1.48	1.01	3.42	0.84	0.66	3.12	1.16	0.84	3.27	77.53
$PM_{2.5}$	tribas	9.03	6.34	3.80	6.81	4.97	3.52	7.92	5.66	3.66	93.20
PM_{10}		12.81	8.90	3.75	8.13	6.04	4.24	10.47	7.47	3.99	74.70
NO_X		5.13	3.21	6.98	3.68	2.37	6.53	4.41	2.79	6.75	72.29
SO_2		1.49	1.01	3.36	0.84	0.65	2.94	1.16	0.83	3.15	80.35

Noted: Yellow highlight represent the lowest value of each information pollution, accuracy measurement, and elapsed time.

The cascade feed forward neural network model differs only when determining the input variables. During the simulation, we constructed the input by vector autoregression. Then, we considered the input as the lag variable of each predicted variable, in this case, the air pollution data at the four locations of Taichung, Taipei, Hsinchu, and Kaohsiung. Then, in the CFNN model for the four locations, neurons were compiled in the layer and the signal from the input to the first input layer, then to the second layer (hidden layer), and finally to the output layer. The general equation for forecasting pollution data in the four locations, represented in Equation (19), was used for prediction purposes in these study areas. Meanwhile, Equation (20) shows four input neurons Y_{t-1} (lag 1) and five neurons in hidden layer of Z_t. To perform the forecasting, we used Equation (21) for NO_x with the radial basis activation function, Equation (22) for $PM_{2.5}$ with the SoftMax activation function, Equation (20) for PM_{10} with the logsig activation function, and Equation (23) for SO_2 with the tribas activation function. We provide the results of forecasting in Figure 7 for the next 30 steps. The results show Taichung constantly leading with the highest pollutant score compared to other cities in Taiwan.

$$\begin{aligned} \hat{Y}_t &= \psi_2\left\{[w_{b0}\ w_0\ w_{i2}]\begin{bmatrix}1\\ Z_t\\ Y_{t-1}\end{bmatrix}\right\} \\ Z_t &= \psi_2\left(\begin{bmatrix} w_{bi} & w_{i1}\end{bmatrix}\begin{bmatrix}1\\ Y_{t-1}\end{bmatrix}\right) \end{aligned} \tag{19}$$

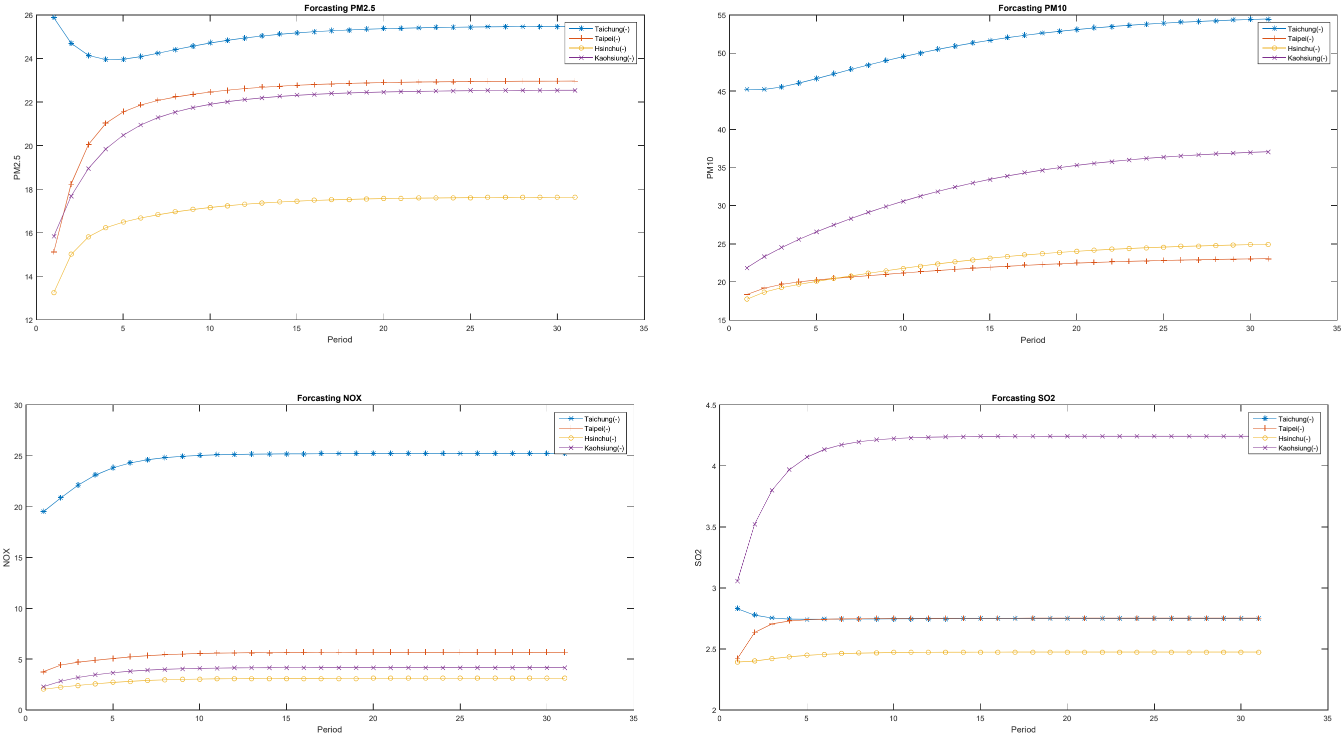

Figure 7. Forecasting all pollution datasets using the CFNN with a genetic algorithm and backpropagation.

Cascade Neural Network Genetic Algorithm for NO_x using the radial basis activation function:

$$\hat{Y}_t = \begin{bmatrix} -0.1244 & -0.0992 & 0.01054 & -7.4544 & 0.2238 & -6.9588 & 0.5603 & 0.0444 & -0.0689 & 0.0770 \\ -0.2483 & 0.0359 & -0.0665 & -6.6298 & 1.0709 & -1.7180 & 0.0655 & 0.2562 & 0.3422 & 0.0572 \\ -0.4328 & 0.0253 & -0.0226 & 4.9796 & 0.8715 & 5.0640 & 0.1253 & 0.0189 & 0.3570 & 0.0742 \\ -0.2772 & 0.0015 & 0.1201 & -4.45319 & -0.1428 & 4.9089 & 0.1066 & 0.0465 & -0.0148 & 0.5544 \end{bmatrix} \begin{bmatrix} 1 \\ Z_1 \\ Z_2 \\ Z_3 \\ Z_4 \\ Z_5 \\ Y_{1,t-1} \\ Y_{2,t-1} \\ Y_{3,t-1} \\ Y_{4,t-1} \end{bmatrix},$$

$$Z_t = radbas\begin{bmatrix} 5.0776 & 6.4191 & 0.0893 & 0.7930 & -0.2450 \\ 0.8287 & 4.8674 & -2.4160 & -3.1740 & -0.7644 \\ -6.9722 & -4.2852 & 9.1216 & -3.0205 & 8.5264 \\ -9.6954 & -12.9182 & 5.3748 & 18.2621 & -5.5156 \\ 7.7948 & 2.5076 & 2.6535 & -9.1934 & -9.4768 \end{bmatrix}\begin{bmatrix} 1 \\ Y_{1,t-1} \\ Y_{2,t-1} \\ Y_{3,t-1} \\ Y_{4,t-1} \end{bmatrix} \tag{20}$$

Cascade Neural Network Genetic Algorithm for $PM_{2.5}$ using the SoftMax activation function:

$$\begin{bmatrix} 0.9653 & -1.0657 & 3.2999 & -2.4456 & -0.7936 & -1.1990 & 0.7359 & 0.0491 & -0.0690 & 0.1124 \\ 1.2965 & -1.5045 & 2.3489 & 2.0493 & -1.9046 & -1.6001 & 0.0225 & 0.2826 & 0.3253 & 0.0500 \\ 6.0285 & -6.1880 & 0.3716 & 2.3998 & -6.8009 & -6.3181 & 0.1929 & -0.0279 & 0.4639 & 0.1170 \\ 0.9319 & -0.9456 & 10.3730 & 3.4200 & -1.1032 & -0.9099 & 0.0890 & 0.0227 & 0.0463 & 0.7191 \end{bmatrix}\begin{bmatrix} 1 \\ Z_1 \\ Z_2 \\ Z_3 \\ Z_4 \\ Z_5 \\ Y_{1,t-1} \\ Y_{2,t-1} \\ Y_{3,t-1} \\ Y_{4,t-1} \end{bmatrix},$$

$$Z_t = softmax\begin{bmatrix} 6.2714 & -7.3511 & -7.8139 & -1.9507 & 4.3787 \\ -5.6864 & -7.7599 & -8.3507 & -2.9367 & -2.3266 \\ -6.4463 & -6.6875 & 5.0926 & 1.5264 & -1.1062 \\ -5.0961 & -3.3109 & 5.3424 & 6.5753 & -3.4388 \\ 3.6740 & -2.6485 & -6.2284 & -6.7208 & 4.4362 \end{bmatrix}\begin{bmatrix} 1 \\ Y_{1,t-1} \\ Y_{2,t-1} \\ Y_{3,t-1} \\ Y_{4,t-1} \end{bmatrix} \tag{21}$$

Cascade Neural Network Genetic Algorithm for PM_{10} using the logsig activation function:

$$\hat{\mathbf{Y}}_t = \begin{bmatrix} 4.7332 & -0.0171 & -4.7892 & -0.0294 & -0.0499 & -0.0380 & 0.5673 & 0.0698 & 0.0402 & 0.0720 \\ -4.7021 & 0.0480 & 4.5307 & -0.0609 & 0.0313 & -0.1244 & 0.1252 & 0.3677 & 0.1878 & 0.0614 \\ 2.2770 & 0.0263 & -2.4010 & -0.0006 & -0.0102 & 0.0014 & 0.2351 & -0.0648 & 0.5960 & 0.0696 \\ 1.5241 & -0.0534 & -1.4885 & 0.0533 & -0.1240 & 0.1097 & 0.1118 & 0.1017 & 0.1786 & 0.5507 \end{bmatrix}\begin{bmatrix} 1 \\ Z_1 \\ Z_2 \\ Z_3 \\ Z_4 \\ Z_5 \\ Y_{1,t-1} \\ Y_{2,t-1} \\ Y_{3,t-1} \\ Y_{4,t-1} \end{bmatrix},$$

$$Z_t = logsig\begin{bmatrix} -7.6484 & -5.6012 & 5.5769 & 0.2050 & -7.1292 \\ 9.0472 & -2.0909 & -7.4709 & 4.9145 & -5.3312 \\ -4.1385 & -9.9840 & -3.4291 & 6.0077 & 2.4277 \\ -1.5068 & -4.0147 & 3.5676 & 5.6306 & -9.0051 \\ -5.6488 & 5.5027 & 6.1290 & 7.2003 & 6.3822 \end{bmatrix}\begin{bmatrix} 1 \\ Y_{1,t-1} \\ Y_{2,t-1} \\ Y_{3,t-1} \\ Y_{4,t-1} \end{bmatrix} \tag{22}$$

Cascade Neural Network Genetic Algorithm for SO_{10} using the tribas activation function:

$$\hat{Y}_t = \begin{bmatrix} -0.1116 & 5.1674 & -0.0036 & -0.0166 & -3.4727 & -0.2061 & 0.4570 & 0.0222 & 0.0743 & 0.0524 \\ -0.2789 & -1.0341 & -0.0087 & -0.0114 & 7.8267 & 0.1241 & 0.0817 & 0.3550 & 0.1215 & 0.0309 \\ -0.8104 & -7.8058 & -0.0085 & 0.0234 & 5.2240 & 0.0292 & 0.1364 & 0.0647 & 0.4179 & 0.1027 \\ -0.1772 & 6.5887 & -0.0242 & -0.0490 & 6.7444 & 0.0271 & 0.0246 & 0.0067 & 0.0693 & 0.6512 \end{bmatrix} \begin{bmatrix} 1 \\ Z_1 \\ Z_2 \\ Z_3 \\ Z_4 \\ Z_5 \\ Y_{1,t-1} \\ Y_{2,t-1} \\ Y_{3,t-1} \\ Y_{4,t-1} \end{bmatrix},$$

$$Z_t = tribas \begin{bmatrix} 7.3483 & -2.1911 & -8.1641 & 0.4300 & -3.6214 \\ -1.5728 & -2.5029 & -10.1020 & 0.5066 & 7.0828 \\ -5.3810 & -9.9016 & 7.7806 & -2.1473 & 5.0866 \\ -1.1201 & 10.2142 & 6.6401 & 6.7203 & 4.0480 \\ -2.9485 & 8.1185 & 7.2550 & 8.2102 & -8.3387 \end{bmatrix} \begin{bmatrix} 1 \\ Y_{1,t-1} \\ Y_{2,t-1} \\ Y_{3,t-1} \\ Y_{4,t-1} \end{bmatrix} \tag{23}$$

4. Conclusions

In this paper, we first presented a full review of a cascade neural network with a genetic algorithm as applied to space–time forecasting. Experimental results on an air pollution dataset showed that our hybrid methods provide high accuracy as proved by the RMSE, MAE, and sMAPE values. Attributable to its rapid urbanization and industrialization over the last decades, Taiwan faces serious environmental issues, including air pollution. In order to resolve air quality issues, the government has taken several countermeasures. The attempt to eliminate SO_2 and overall suspended particulate matter was very effective when ever-increasing cars threatened city atmospheres with NOx and particulates. A space–time air pollution analysis over the last 10 years using the monitoring data clearly showed that with urban planning and countermeasure policies, air quality has improved. The analysis should be used to make future policy decisions. Air pollution temporal features were examined herein for Taiwan. The pattern from pollutants to particulates differs in air quality for each location. In a nutshell, the PM, SO_2, and NO_x levels have drastically increased. Future research should examine using VAR-SARIMA, VAR-ARCH, and other traditional time series as input.

Author Contributions: Conceptualization, R.E.C., H.Y.; methodology, R.E.C., H.Y.; software, R.E.C., H.Y.; validation, R.E.C., H.Y.; formal analysis, R.E.C., H.Y.; investigation, R.E.C., H.Y.; resources, R.E.C., H.Y.; Writing—original draft, R.E.C., H.Y.; writing—review and editing, R.E.C., H.Y.; visualization, R.E.C., H.Y.; supervision, R.E.C., H.Y., R.-C.C., M.B.; project administration, R.E.C., H.Y., R.-C.C., N.E.G., B.D.S., T.T., M.B., P.U.G., B.P.; funding acquisition, R.E.C., R.-C.C., T.T., M.B. All authors have read and agreed to the published version of the manuscript.

Funding: This research fully supported by Faculty of Business and Economics, University of Indonesia. This research is part of Ministry of Science and Technology, Taiwan [MOST-109-2622-E-324-004]. This research is part of Chaoyang University of Technology and the Higher Education Sprout Project, Ministry of Education (MOE), Taiwan, under the project name: "The R&D and the cultivation of talent for health-enhancement products". This research is fully supported by the Directorate General of Research and Community Service, the Ministry of Research, and Technology/National Agency for Research and Innovation of the Republic of Indonesia through World-Class Research Program 2021.

Institutional Review Board Statement: Not applicable.

Informed Consent Statement: Not applicable.

Data Availability Statement: Supplementary code to this article can be found online at https://github.com/Rezzy94/cascadenn (accessed on 1 May 2021). The copyright of this programming was officially registered on May 31, 2021, by the Directorate General of Intellectual Property—Ministry of Law and Human Rights, the Republic of Indonesia, with the registration number [EC00202125523] and [000252427], valid for 50 (fifty) years from the first announcement of the work. This copyright registration letter or related rights products are in accordance with article 72 of law number 28 of 2014 concerning copyright.

Conflicts of Interest: The authors declare no conflict of interest.

Abbreviations

VAR: vector autoregression, GA: genetic algorithm, FFNN: feedforward neural network, MAE: mean absolute error, sMAPE: symmetric mean absolute percentage error, RMSE: root-mean-square error, MAE: mean absolute error, $PM_{2.5}$: fine particulate matter with a diameter of 2.5 µm, PM_{10}: fine particulate matter 10 micrometers or less in diameter, SO_2: sulfur dioxide, NO_x: nitrogen dioxide, BP: backpropagation.

References

1. Querol, X.; Alastuey, A.; Ruiz, C.R.; Artiñano, B.; Hansson, H.C.; Harrison, R.M.; Buringh, E.; Ten Brink, H.M.; Lutz, M.; Bruckmann, P.; et al. Speciation and origin of PM10 and PM2.5 in selected European cities. *Atmos. Environ.* **2004**, *38*, 6547–6555. [CrossRef]
2. Fan, J.; Wu, L.; Ma, X.; Zhou, H.; Zhang, F. Hybrid support vector machines with heuristic algorithms for prediction of daily diffuse solar radiation in air-polluted regions. *Renew. Energy* **2020**, *145*, 2034–2045. [CrossRef]
3. Masseran, N.; Safari, M.A.M. Intensity–duration–frequency approach for risk assessment of air pollution events. *J. Environ. Manag.* **2020**, *264*, 110429. [CrossRef] [PubMed]
4. Masseran, N.; Safari, M.A.M. Modeling the transition behaviors of PM 10 pollution index. *Environ. Monit. Assess.* **2020**, *192*, 441. [CrossRef] [PubMed]
5. De Vito, S.; Piga, M.; Martinotto, L.; Di Francia, G. CO, NO_2 and NOx urban pollution monitoring with on-field calibrated electronic nose by automatic bayesian regularization. *Sens. Actuators B Chem.* **2009**, *143*, 182–191. [CrossRef]
6. Winarso, K.; Yasin, H. Modeling of air pollutants SO_2 elements using geographically weighted regression (GWR), geographically temporal weighted regression (GTWR) and mixed geographically temporalweighted regression (MGTWR). *ARPN J. Eng. Appl. Sci.* **2016**, *11*, 8080–8084.
7. Zhang, J.J.; Wei, Y.; Fang, Z. Ozone pollution: A major health hazard worldwide. *Front. Immunol.* **2019**, *10*, 2518. [CrossRef]
8. Bernstein, J.A.; Alexis, N.; Barnes, C.; Bernstein, I.L.; Bernstein, J.A.; Nel, A.; Peden, D.; Diaz-Sanchez, D.; Tarlo, S.M.; Williams, P.B. Health effects of air pollution. *J. Allergy Clin. Immunol.* **2004**, *114*, 1116–1123. [CrossRef]
9. Xing, Y.F.; Xu, Y.H.; Shi, M.H.; Lian, Y.X. The impact of PM2.5 on the human respiratory system. *J. Thorac. Dis.* **2016**, *8*, E69–E74.
10. Rossati, A. Global warming and its health impact. *Int. J. Occup. Environ. Med.* **2017**, *8*, 7–20. [CrossRef]
11. Suhartono, S.; Subanar, S. Development of model building procedures in wavelet neural networks for forecasting non-stationary time series. *Eur. J. Sci. Res.* **2009**, *34*, 416–427.
12. Suhermi, N.; Suhartono; Prastyo, D.D.; Ali, B. Roll motion prediction using a hybrid deep learning and ARIMA model. *Procedia Comput. Sci.* **2018**, *144*, 251–258. [CrossRef]
13. McCulloch, W.S.; Pitts, W. A logical calculus of the ideas immanent in nervous activity. *Bull. Math. Biophys.* **1943**, *5*, 115–133. [CrossRef]
14. Chen, R.C.; Dewi, C.; Huang, S.W.; Caraka, R.E. Selecting critical features for data classification based on machine learning methods. *J. Big Data* **2020**, *7*, 52. [CrossRef]
15. Caraka, R.E.; Lee, Y.; Chen, R.C.; Toharudin, T. Using Hierarchical Likelihood towards Support Vector Machine: Theory and Its Application. *IEEE Access* **2020**, *8*, 194795–194807. [CrossRef]
16. Mueller, J.-A.; Lemke, F. Self-Organising Data Mining: An Intelligent Approach to Extract Knowledge from Data. 1999. Available online: https://www.knowledgeminer.eu/pdf/sodm.pdf (accessed on 6 May 2021).
17. De Gooijer, J.G.; Hyndman, R.J. 25 years of time series forecasting. *Int. J. Forecast.* **2006**, *22*, 443–473. [CrossRef]
18. Kaimian, H.; Li, Q.; Wu, C.; Qi, Y.; Mo, Y.; Chen, G.; Zhang, X.; Sachdeva, S. Evaluation of different machine learning approaches to forecasting PM2.5 mass concentrations. *Aerosol Air Qual. Res.* **2019**, *19*, 1400–1410. [CrossRef]
19. Guo, Y.; Liu, Y.; Oerlemans, A.; Lao, S.; Wu, S.; Lew, M.S. Deep learning for visual understanding: A review. *Neurocomputing* **2016**, *187*, 27–48. [CrossRef]
20. Szandała, T. Review and comparison of commonly used activation functions for deep neural networks. *arXiv* **2020**. Available online: https://arxiv.org/abs/2010.09458 (accessed on 6 May 2021).
21. Sony, S.; Dunphy, K.; Sadhu, A.; Capretz, M. A systematic review of convolutional neural network-based structural condition assessment techniques. *Eng. Struct.* **2021**, *226*, 111347. [CrossRef]
22. Caraka, R.E.; Chen, R.C.; Yasin, H.; Pardamean, B.; Toharudin, T.; Wu, S.H. Prediction of Status Particulate Matter 2.5 using State Markov Chain Stochastic Process and HYBRID VAR-NN-PSO. *IEEE Access* **2019**, *7*, 161654–161665. [CrossRef]
23. Kuster, C.; Rezgui, Y.; Mourshed, M. Electrical load forecasting models: A critical systematic review. *Sustain. Cities Soc.* **2017**, *35*, 257–270. [CrossRef]

24. Cios, K.J.; Pedrycz, W.; Swiniarski, R.W.; Kurgan, L.A. *Data Mining: A Knowledge Discovery Approach*; Springer: Boston, MA, USA, 2007; ISBN 9780387333335.
25. Makridakis, S.; Spiliotis, E.; Assimakopoulos, V. The M4 Competition: 100,000 time series and 61 forecasting methods. *Int. J. Forecast.* **2020**, *36*, 54–74. [CrossRef]
26. Makridakis, S.G.; Wheelwright, S.C.; Hyndman, R.J. Forecasting: Methods and Applications. *J. Forecast.* **1998**, 1–656. [CrossRef]
27. Wong, K.W.; Wong, P.M.; Gedeon, T.D.; Fung, C.C. Rainfall prediction model using soft computing technique. *Soft Comput.* **2003**, *7*, 434–438. [CrossRef]
28. Hochreiter, S.; Schmidhuber, J. Long Short-Term Memory. *Neural Comput.* **1997**, *9*, 1735–1780. [CrossRef] [PubMed]
29. Mislan, M.; Haviluddin, H.; Hardwinarto, S.; Sumaryono, S.; Aipassa, M. Rainfall Monthly Prediction Based on Artificial Neural Network: A Case Study in Tenggarong Station, East Kalimantan—Indonesia. *Procedia Comput. Sci.* **2015**, *59*, 142–151. [CrossRef]
30. Darwin, C. *The Correspondence of Charles Darwin: 1821–1860*; Cambridge University Press: Cambridge, UK, 2002.
31. Pfeiffer, J.R. Evolutionary theory. In *George Bernard Shaw in Context*; Cambridge University Press: Cambridge, UK, 2015; ISBN 9781107239081.
32. Wuketits, F.M. Charles darwin and modern moral philosophy. *Ludus Vitalis* **2009**, *17*, 395–404.
33. García-Martínez, C.; Rodriguez, F.J.; Lozano, M. Genetic algorithms. In *Handbook of Heuristics*; Springer: Cham, Switzerland, 2018; ISBN 9783319071244. Available online: https://www.springer.com/gp/book/9783319071237 (accessed on 6 May 2021).
34. Sivanandam, S.; Deepa, S. *Introduction to Genetic Algorithms*; Springer: Berlin/Heidelberg, Germany, 2008.
35. Gupta, J.N.D.; Sexton, R.S. Comparing backpropagation with a genetic algorithm for neural network training. *Omega* **1999**, *27*, 679–684. [CrossRef]
36. Caraka, R.E.; Chen, R.C.; Yasin, H.; Lee, Y.; Pardamean, B. Hybrid Vector Autoregression Feedforward Neural Network with Genetic Algorithm Model for Forecasting Space-Time Pollution Data. *Indones. J. Sci. Technol.* **2021**, *6*, 243–266.
37. Kubat, M.; Kubat, M. The Genetic Algorithm. In *An Introduction to Machine Learning*; Springer International Publishing: Cham, Switzerland, 2017.
38. Moscato, P.; Cotta, C. A Modern Introduction to Memetic Algorithms. In *Handbook of Metaheuristics*; Springer: Boston, MA, USA, 2010; pp. 141–183. Available online: https://link.springer.com/chapter/10.1007/978-1-4419-1665-5_6 (accessed on 6 May 2021).
39. Makridakis, S.; Wheelwright, S.C. Forecasting Methods for Management. *Oper. Res. Q.* **1974**, *25*, 648–649. [CrossRef]
40. Makridakis, S. A Survey of Time Series. *Int. Stat. Rev. Rev. Int. Stat.* **1976**, *44*, 29. [CrossRef]
41. Warsito, B.; Santoso, R.; Suparti; Yasin, H. Cascade Forward Neural Network for Time Series Prediction. *J. Phys. Conf. Ser.* **2018**, *1025*, 012097. [CrossRef]
42. Schetinin, V. A learning algorithm for evolving cascade neural networks. *Neural Process. Lett.* **2003**, *17*, 21–31. [CrossRef]
43. Ding, S.; Zhao, H.; Zhang, Y.; Xu, X.; Nie, R. Extreme learning machine: Algorithm, theory and applications. *Artif. Intell. Rev.* **2015**, *44*, 103–115. [CrossRef]
44. Suhartono; Prastyo, D.D.; Kuswanto, H.; Lee, M.H. Comparison between VAR, GSTAR, FFNN-VAR and FFNN-GSTAR Models for Forecasting Oil Production Methods. *Mat. Malays. J. Ind. Appl. Math.* **2018**, *34*, 103–111.
45. Prastyo, D.D.; Nabila, F.S.; Lee, M.H.S.; Suhermi, N.; Fam, S.F. VAR and GSTAR-based feature selection in support vector regression for multivariate spatio-temporal forecasting. In *Communications in Computer and Information Science*; Springer: Singapore, 2018; pp. 46–57.
46. Zhang, P.G. Time series forecasting using a hybrid ARIMA and neural network model. *Neurocomputing* **2003**, *50*, 159–175. [CrossRef]
47. Geurts, M.; Box, G.E.P.; Jenkins, G.M. Time Series Analysis: Forecasting and Control. *J. Mark. Res.* **2006**. [CrossRef]
48. McLeod, A.I.; Yu, H.; Mahdi, E. Time Series Analysis with R. *Handb. Stat.* **2011**, *30*, 661–672. [CrossRef]
49. Liao, W.T. Clustering of time series data—A survey. *Pattern Recognit.* **2005**, *38*, 1857–1874. [CrossRef]
50. Subba Rao, T. Time Series Analysis. *J. Time Ser. Anal.* **2010**, *31*, 139. [CrossRef]
51. Mudelsee, M. *Climate Time Series Analysis: Regression*; Springer: Dordrecht, The Netherlands, 2010; Volume 42, ISBN 978-90-481-9481-0.
52. Zhu, X.; Pan, R.; Li, G.; Liu, Y.; Wang, H. Network vector autoregression. *Ann. Stat.* **2017**, *45*, 1096–1123. [CrossRef]
53. Nourani, V.; Baghanam, A.H.; Adamowski, J.; Gebremichael, M. Using self-organizing maps and wavelet transforms for space-time pre-processing of satellite precipitation and runoff data in neural network based rainfall-runoff modeling. *J. Hydrol.* **2013**, *476*, 228–243. [CrossRef]
54. Ippoliti, L.; Valentini, P.; Gamerman, D. Space-time modelling of coupled spatiotemporal environmental variables. *J. R. Stat. Soc. Ser. C Appl. Stat.* **2012**. [CrossRef]
55. Sharma, S.; Sharma, S. Understanding Activation Functions in Neural Networks. *Int. J. Eng. Appl. Sci. Technol.* **2017**, *4*, 310–316.
56. Apicella, A.; Donnarumma, F.; Isgrò, F.; Prevete, R. A survey on modern trainable activation functions. *Neural Netw.* **2021**, *138*, 14–32. [CrossRef]
57. Al-Rikabi, H.M.H.; Al-Ja'afari, M.A.M.; Ali, A.H.; Abdulwahed, S.H. Generic model implementation of deep neural network activation functions using GWO-optimized SCPWL model on FPGA. *Microprocess. Microsyst.* **2020**, *77*, 103141. [CrossRef]

58. Boob, D.; Dey, S.S.; Lan, G. Complexity of training ReLU neural network. *Discret. Optim.* **2020**, 100620. [CrossRef]
59. Liu, B. Understanding the loss landscape of one-hidden-layer ReLU networks. *Knowl. Based Syst.* **2021**, *220*, 106923. [CrossRef]
60. Bouwmans, T.; Javed, S.; Sultana, M.; Jung, S.K. Deep neural network concepts for background subtraction: A systematic review and comparative evaluation. *Neural Netw.* **2019**, *117*, 8–66. [CrossRef]